

EUROPEAN SPACE AGENCY

Giovanna De Chiara

**TRACKING A TROPICAL CYCLONE
WITH ERS-SCAT:
A CMOD4 MODEL REVIEW**

Acknowledgments

This technical report describes the work carried out during my traineeship at ESRIN from January 2001 to July 2001.

I would like to take the opportunity to thank my tutor Pascal Lecomte for the total support and the essential comments for the work.

I am very grateful to Raffaele Crapolicchio for the suggestions, the constant assistance and the time that he spent with me.

Finally I would like to thank Lidia Saavedra De Miguel for her encouragement and the colleagues that provide me the total support I needed in this period.

G. De Chiara

CONTENTS

Abstract

1	The CMOD4 model	
	1.1: The scatterometer.....	1
	1.2: The CMOD4 model.....	4
2	The tropical cyclone.....	19
3	Experiments	
	3.1: Premise.....	23
	3.2: Theoretical facts.....	24
	3.3: Experimental facts.....	30
4	Concluding remarks.....	45
	References.....	46

Abstract

The spaceborne scatterometer is a microwave radar that provides high precision radiometric measures of the normalized radar cross section σ^0 of the ocean surface. The backscatter is affected by the superficial roughness that is in turn related to the local wind. Since microwave wavelengths are used the scatterometer, at first order, can be meant as an instrument which provides measurements independent of clouds and sun illumination therefore it is able to observe the internal structure of a Tropical Cyclone (TC).

The relationship between the σ^0 and the surface wind field is described by a geophysical model function (GMF). The model used in the ERS scatterometer processing is the well-known semi-empirical model CMOD4. Unfortunately this model is not tailored for high wind speeds, such as the case of TCs. This fact causes a poor quality in the wind field estimated through the scatterometer data acquired over a TC.

In this report we describe a study in view of a possible extension of the CMOD4 for high wind speeds. The study has been based on the ERS-2 σ^0 measurements relevant to six selected TCs and the corresponding wind speeds obtained by employing the Holland model. We have selected six TCs and for each one we have developed a 3D wind speed pattern making use of the wind speed available through the NHC (National Hurricane Center) warnings. The obtained wind speeds are then correlated to the σ^0 's acquired over these six TCs.

The results obtained in this work support the need to extend the CMOD4 model.

CHAPTER 1

THE CMOD4 MODEL

1.1 The scatterometer

The wind scatterometer is a radar remote sensing instrument which is capable to measure the normalized backscattering σ^0 of the ocean surface with great radiometric accuracy and under multiple observation, i.e. azimuth angles. Physically the sea roughness, which is the major affecting σ^0 , is related to the sea surface wind. By exploiting such a set of measurements and a geophysical model function (GMF) which relates σ^0 to the near surface wind, it is possible to retrieve, i.e. estimate, the surface wind field.

In particular the scatterometer deployed on board of the ERS-2 is composed by three antennas that make almost instantaneous three σ^0 measurements at different azimuth angles.

The ERS-2 scatterometer operates at C band, so the measurements are independent of cloud coverage and sun illumination.

The antennas point to the right of the space-craft in three directions: 45 degrees forward (Forebeam), sideways (Midbeam) and 45 degrees backwards (Aftbeam) with respect to the satellite flight direction (Fig. 1.1).

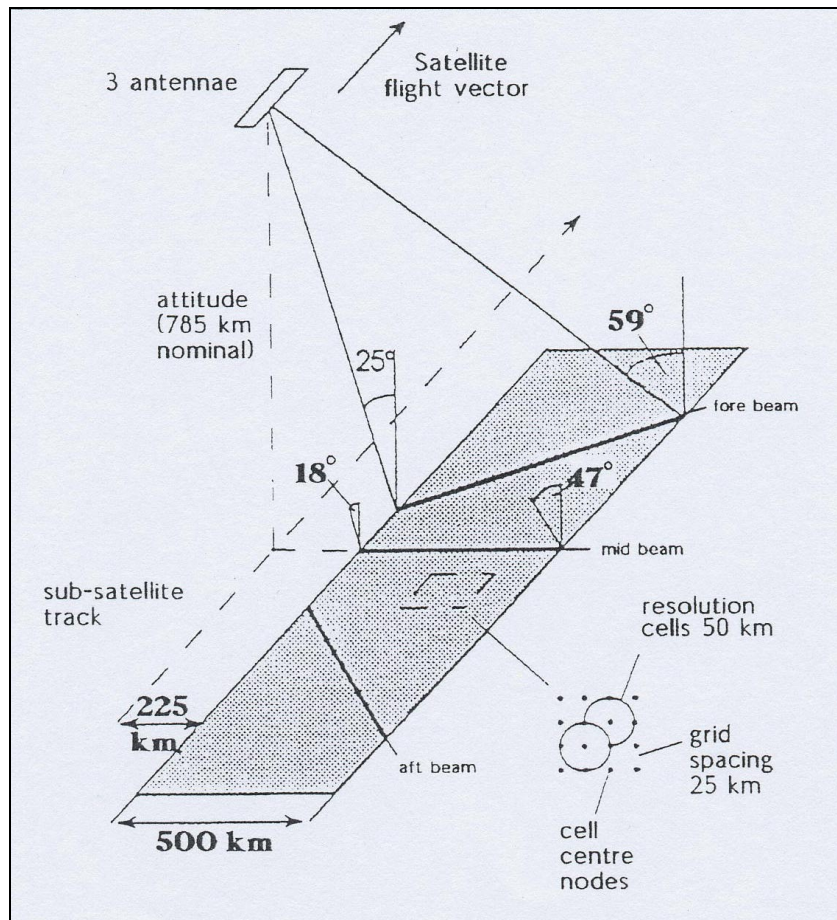


Fig. 1.1: ERS-2 Scatterometer.

The antennas make backscattering measurements at about 50 km of resolution sampled on a 25 km grid. So across the swath there are 19 nodes (Fig. 1.2) and the incidence angle grows for higher nodes.

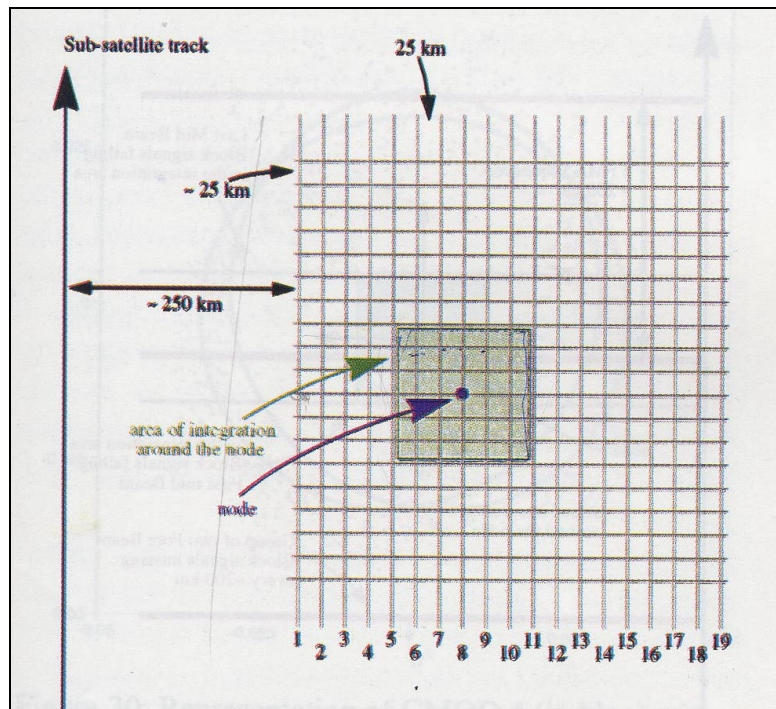


Fig. 1.2: node localitation [Lecomte, 1998].

Each triplet of σ^0 measurements can be plotted in a 3D space, spanned by an axis system representing the fore, mid and aft beam measurements. This space is defined as the σ^0 space measurement.

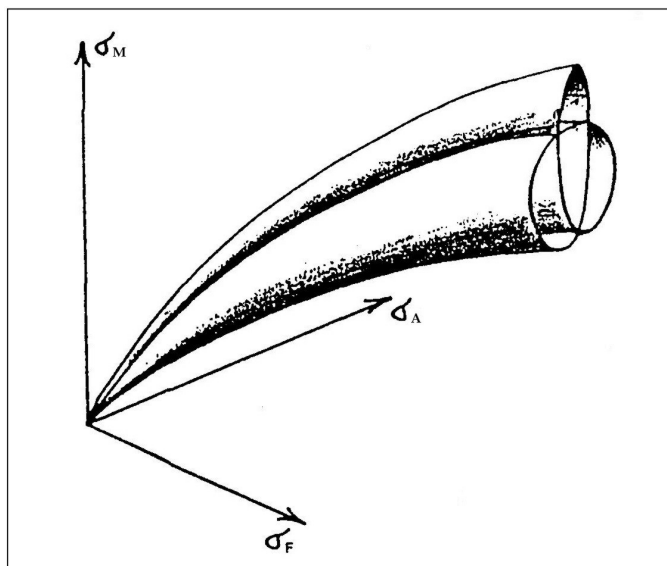


Fig. 1.2: the CMOD4 model [Lecomte, 1998].

For a given node across the swath the measured σ^0 triplets are distributed around a well-defined “conical surface”. This surface consists of two closely overlapping sheaths. One sheath represents upwind conditions, the other sheath corresponds to downwind conditions [Stoffelen, 1998].

Physically, the extension of the cone in the 3D space is related to the amplitude of ocean capillary waves: the lesser the amplitude, the greater the surface roughness and it must be consider greater σ^0 measurement. The diameter of the cone is related to the anisotropy of backscattering of radar waves from the centimeter-wavelength ocean waves: at variance of wind direction varies the sea spectrum in each antenna direction.

In the model this two parameter are connected with the wind speed and direction.

1.2 THE CMOD4 MODEL

The model adopted by ESA since 1993 is called CMOD4 and was derived by Stoffelen and Anderson [Stoffelen, 1998].

The CMOD4 has the form [Stoffelen, 1998]:

$$\sigma_{lin}^0 = b_0 (1 + b_1 \cos \phi + b_3 \tanh b_2 \cos 2\phi)^{1.6}, \quad (1)$$

where

$$b_0 = b_R 10^{\alpha + \gamma \cdot f_1(V + \beta)}, \quad (2)$$

and

$$f_1(s) = \begin{cases} -10, s \leq 10^{-10} \\ \log s, 10^{-10} < s \leq -5 \\ \sqrt{s}/32, s > 5 \end{cases} \quad (3)$$

$\alpha, \beta, \gamma, b_1, b_2$ e b_3 are expanded Legendre polynomials. b_R is the residual correction factor of b_0 and is function of incidence angle.

The parameters are specified as follow [Stoffelen, 1998]:

$$\alpha = c_1 P_0 + c_2 P_1 + c_3 P_2, \quad (4)$$

$$\gamma = c_4 P_0 + c_5 P_1 + c_6 P_2, \quad (5)$$

$$\beta = c_7 P_0 + c_8 P_1 + c_9 P_2, \quad (6)$$

$$b_1 = c_{10} P_0 + c_{11} V + (c_{12} P_0 + c_{13} V) f_2(x), \quad (7)$$

$$b_2 = c_{14} P_0 + c_{15} (1 + P_1) V, \quad (8)$$

$$b_3 = 0.42(1 + c_{16}(c_{17} + x)(c_{18} + V)), \quad (9)$$

$$b_R = LUT(\theta), \quad (10)$$

$$f_2(x) = \tanh\{+ 2.5(x + 0.35)\} - 0.61(x + 0.35), \quad (11)$$

where the Legendre polynomials are $P_0 = 1$, $P_1 = x$ and $P_2 = (3x^2 - 1)/2$ with $x = (\theta - 40)/25$. V is the wind speed in m/s, ϕ the relative wind direction in degrees and θ the incidence angle in degrees.

Parameter	Coefficient	Value	Parameter	Coefficient	Value
α	c ₁	-2.301523	b_1	c ₁₀	0.014430
	c ₂	-1.632686		c ₁₁	0.002484
	c ₃	0.761210		c ₁₂	0.074450
γ	c ₄	1.156619	b_2	c ₁₃	0.004023
	c ₅	0.595955		c ₁₄	0.148810
	c ₆	-0.293819		c ₁₅	0.089286
β	c ₇	-1.015244	b_3	c ₁₆	-0.006667
	c ₈	0.342175		c ₁₇	3.000000
	c ₉	-0.500786		c ₁₈	-10.000000

Tab. 1.1: CMOD4 coefficients [Stoffelen, 1998].

The validity of the model is in the range 2-20 m/s.

Although there is no immediate evidence of saturation of the σ^0 at high wind speed, as speed up to 22 m/s are retrieved and seems reasonable, there is a suggestion that the noise, as measured from the transfer function to the cone surface is higher at high wind speed.

This could indicate a general misfit of the transfer function to the true cone surface or a reduced validity of the two-parameter transfer function [Stoffelen, 1980].

In particular, it seems that CMOD4 underestimates the real high wind speed up to 20 m/s.

To better understand the behaviour of the model and the relation between it and the data now we consider a simplified representation of the cone.

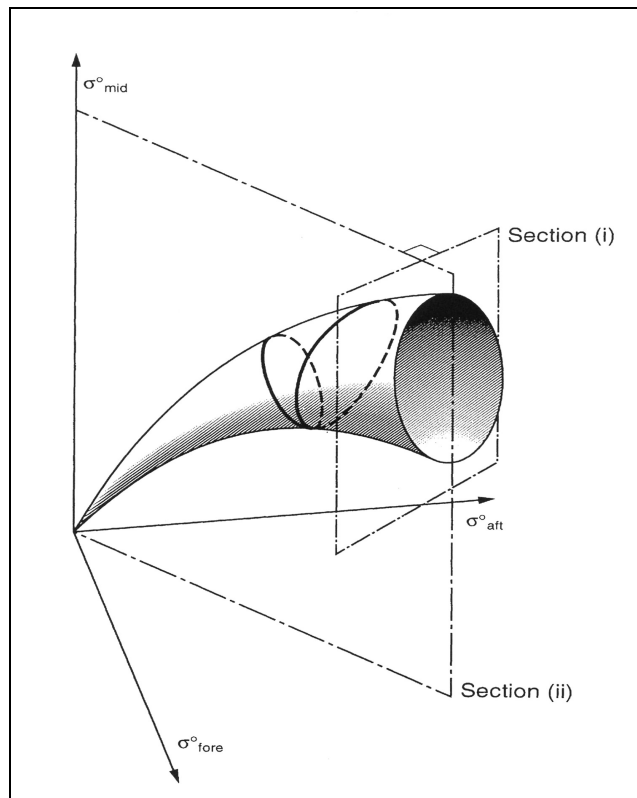


Fig. 1.3: simplified representation of CMOD4 model [Stoffelen, 1998].

The line on the surface is a schematic line of constant wind speed. In particular the fore one is for upwind direction, the rear one for downwind direction.

The σ^0 data set used in this study was selected from the ESA archives files. We chose all files from 20 to 28 February 1999. This choice allows obtaining three global earth coverage.

First we consider the σ^0 measurements with respect to wind direction for a given wind speed verifying the sinusoidal relationship between the two quantities. We report the model with the dotted line and the measures with points.

The direction is always calculated with respect to the mid beam. Each colour shows a wind speed growing from bottom to the top.

In each graphic there are the plot of mid beam in the top, the fore beam in the centre and the aft beam in the bottom (Fig. 1.4). The analysis of the data set show that there is a discrepancy between CMOD4 model and measurements. In particular in Figg. 1.4, 1.6, 1.7 note that the discrepancy is of 10°-15° to the right for the crosswind minimum for the fore beam. The opposite, to the left, for the aft beam. This shift of 15° shows that the σ^0 maximum for the aft beam and the fore beam minimum are not located at 45° and 225° (as for the model) but at about 60° and 240°.

Similarly the aft beam σ^0 minimum and the fore beam σ^0 maximum are not at 135° and 315° but in 120° and 300°.

This discrepancy is unsuspected since the considered wind speed are below 20 m/s.

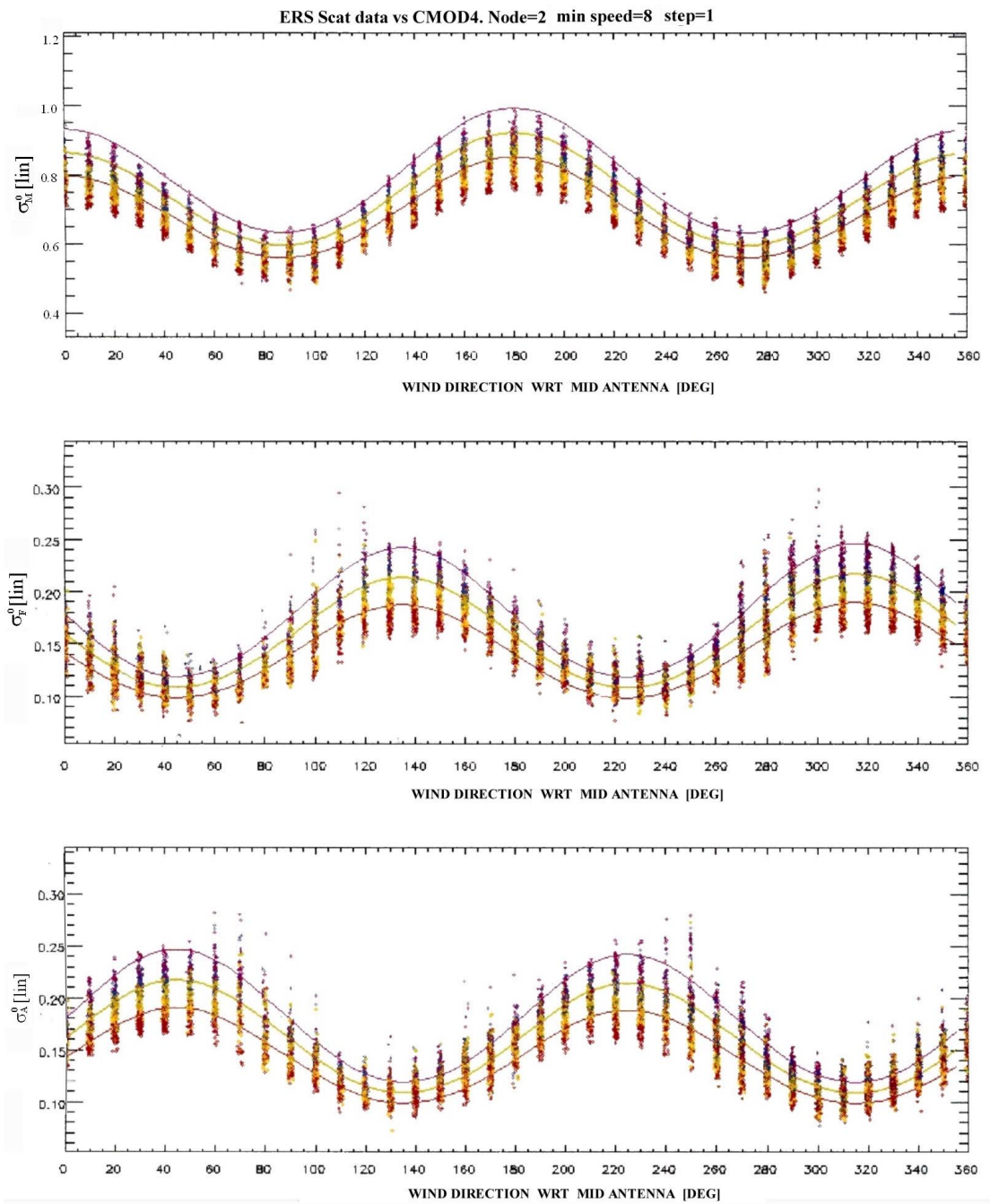


Fig. 1.4: with respect to the wind direction for mid (top), fore (centre) and aft (bottom) beam for node 2. Each wind speed is plotted with different colours. For the model, plotted with the lines, the speeds of 8, 9 and 10 m/s are reported, for data measurements, plotted with points, all speeds from 8 to 10 m/s.

The data shifting is shown for all nodes and is slightly stronger in higher nodes

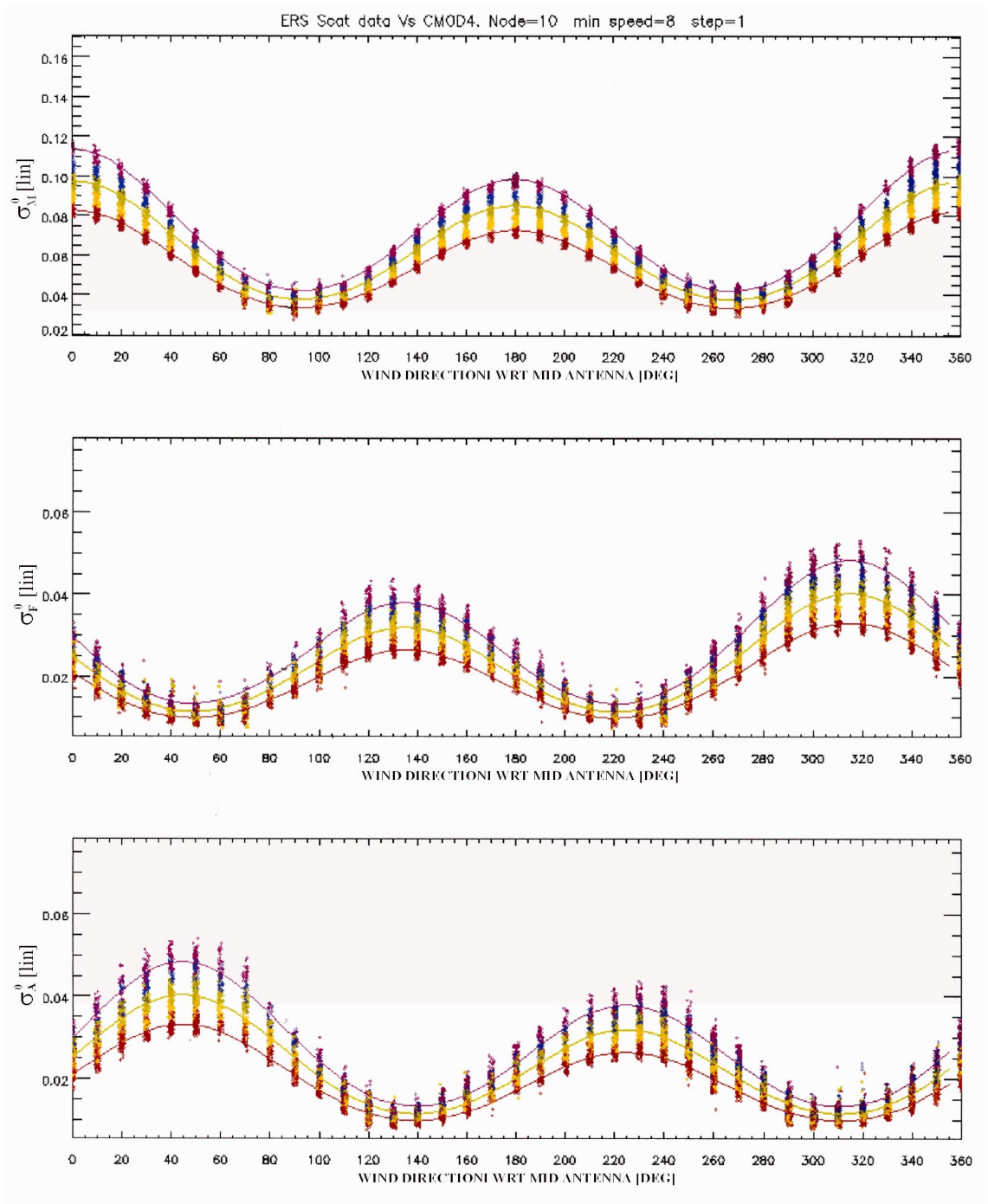


Fig. 1.5: σ^0 with respect to the wind direction for mid (top), fore (centre) and aft (bottom) beam for node 10. Each wind speed is plotted with different colours. For the model, plotted with the lines, the speeds of 8, 9 and 10 m/s are reported, for data measurements, plotted with points, all speeds from 8 to 10 m/s.

With these results, the $\sigma_A^0 - \sigma_F^0$ difference should have the minimum around 135° and 315° and maximum around 60° and 240° . This is confirmed in Fig. 1.6 where the $\sigma_A^0 - \sigma_F^0$ difference with respect to wind direction is plotted.

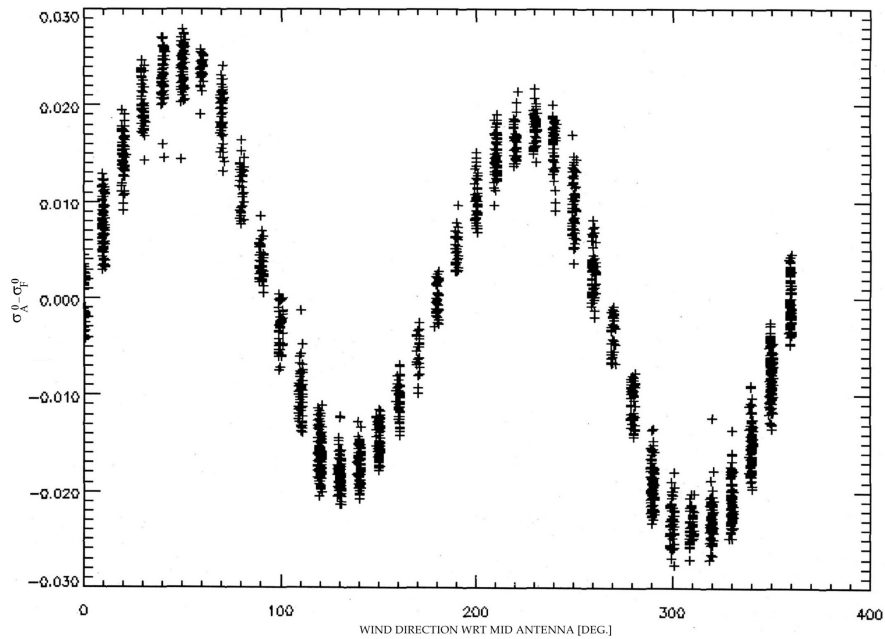


Fig. 1.6: plot of the difference $\sigma_A^0 - \sigma_F^0$ with respect to the wind direction.

Furthermore we can note greater data dispersion with respect to the model for side antennas, for each one in two opposite directions. For the fore beam the scatter is greater around 100° and 280° that is at -25° with respect to upwind and downwind; for the aft beam is at 70° and 250° , at $+25^\circ$ with respect to upwind and downwind. This effect is greater at internal nodes.

For mid antenna measures neither shift nor dispersion is noticed.

For very high wind speed, such as for TC there is also a flattening of data such as is lesser the difference between maximum and minimum. But for

these winds, there aren't many measures and so it's not possible to analyse the phenomena.

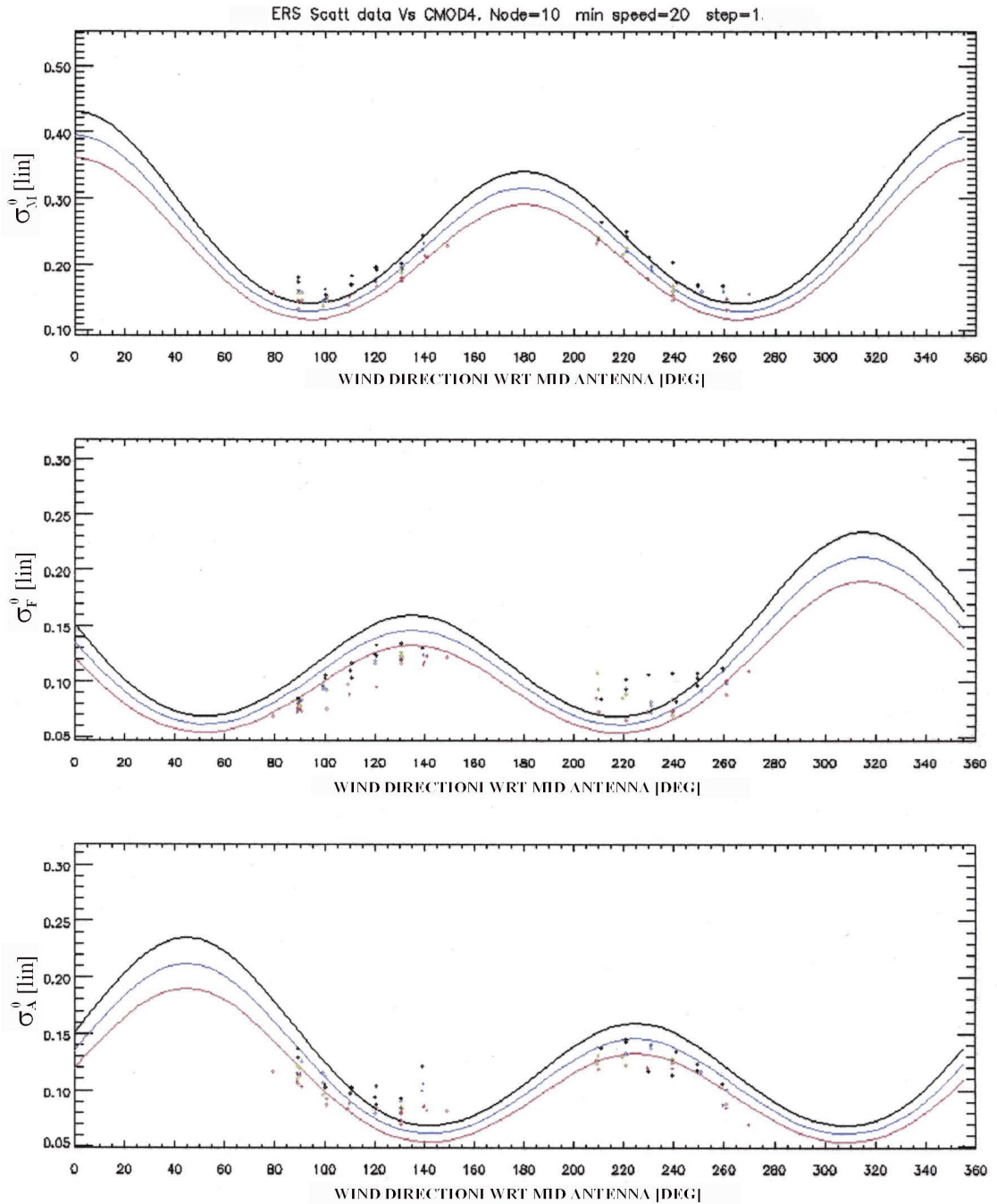


Fig. 1.7: σ^0 with respect to the wind direction for mid (top), fore (centre) and aft (bottom) beam for node 10. Each wind speed is plotted with different colours. For the model, plotted with the lines, the speeds of 20, 21 and 22 m/s are reported, for data measurements, plotted with points, all speeds from 20 to 22 m/s.

As shown in Fig. 1.3 the σ^0 triplets with the same wind speed lie on the two circumferences, one for upwind and the other for downwind. We can represent the σ^0 measures and the CMOD4 model for the same wind speed projected on the plane $\left(\left[\sigma_A^0 - \sigma_F^0 \right] / \sqrt{2}; \sigma_M^0 - \bar{\sigma}_M^0 \right)$.

The colour changes around the circumference showing the changes in wind direction; each colour shade indicates 10° of direction. The colour black is centred on 0° , then passing by the purple we arrive on the blue in 90° . The sky-blue is for 180° , the green for 270° .

First we can see that for a given node growing the wind speed grows the diameter. For internal nodes the upwind values are greater than downwind ones, otherwise for central and external nodes.

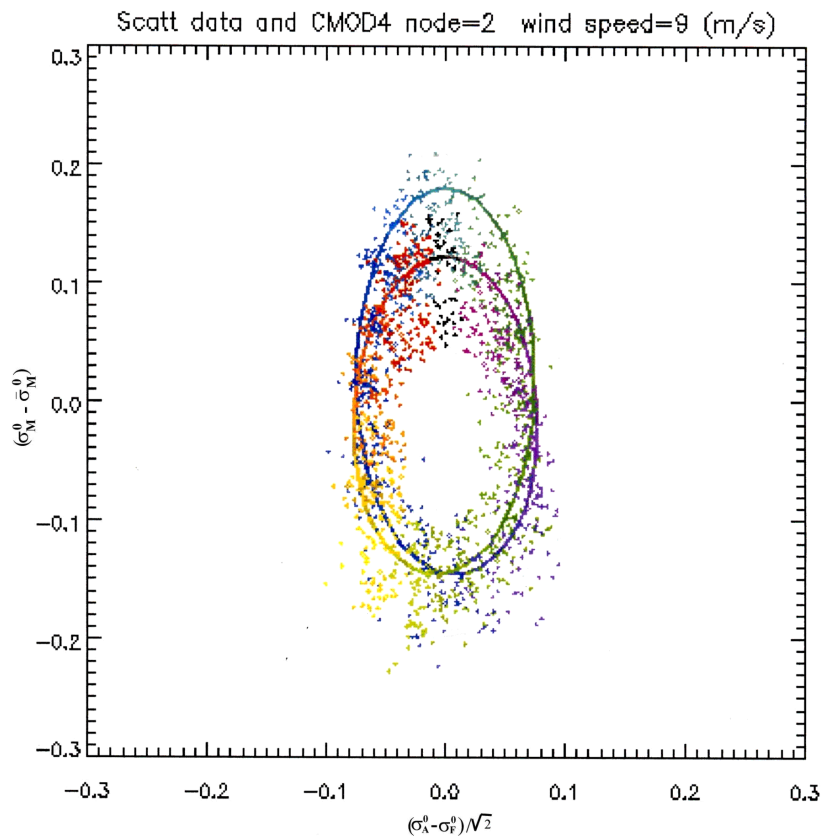


Fig. 1.8: section of CMOD4 and σ^0 measurements for node 2 and wind speed of 9 m/s.

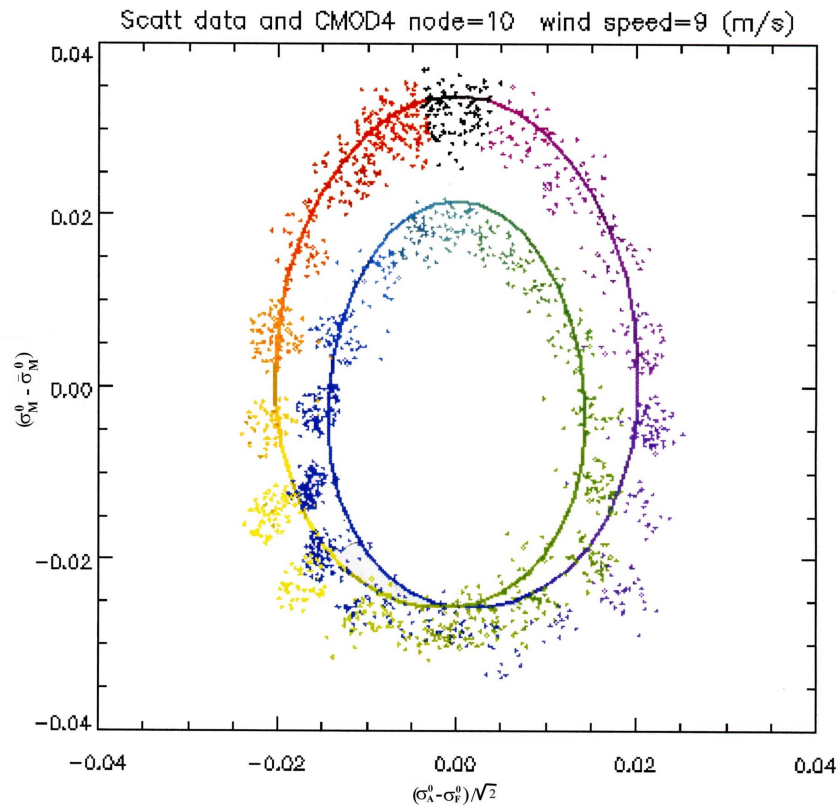


Fig. 1.9: section of CMOD4 and σ^0 measurements for node 10 and wind speed of 9 m/s.

Generally we can say that data is more or less centred on the model for upwind and downwind values. Crosswind measurements show a trend less roundness than CMOD4 such as for these directions the model must have a lesser roundness shape. This is more evident in Fig. 1.9. this data analysis is congruent to what stated at pag. 10.

The $\sigma_A^0 - \sigma_F^0$ minimum and maximum, indicated in 135° , 315° , 60° and 240° , in this plot correspond to the blue, yellow, purple and green points that, in fact, are larger than the model. Also the greater scatter of data mentioned previously confirm the new model shape because for fore beam the greater scatter in 100° and 280° directions cause a shift of blue

and yellow measures; for aft beam the dispersion in 70° and 250° corresponds to purple and green points.

As the two circumferences don't lie on the same plane we can analyze the position of the measures with respect to CMOD4 in the symmetric plane

$\left[(\sigma_A^0 + \sigma_F^0)\sqrt{2}; \sigma_M^0 \right]$ and from the top in the plane $\sigma_A^0 \sigma_F^0$.

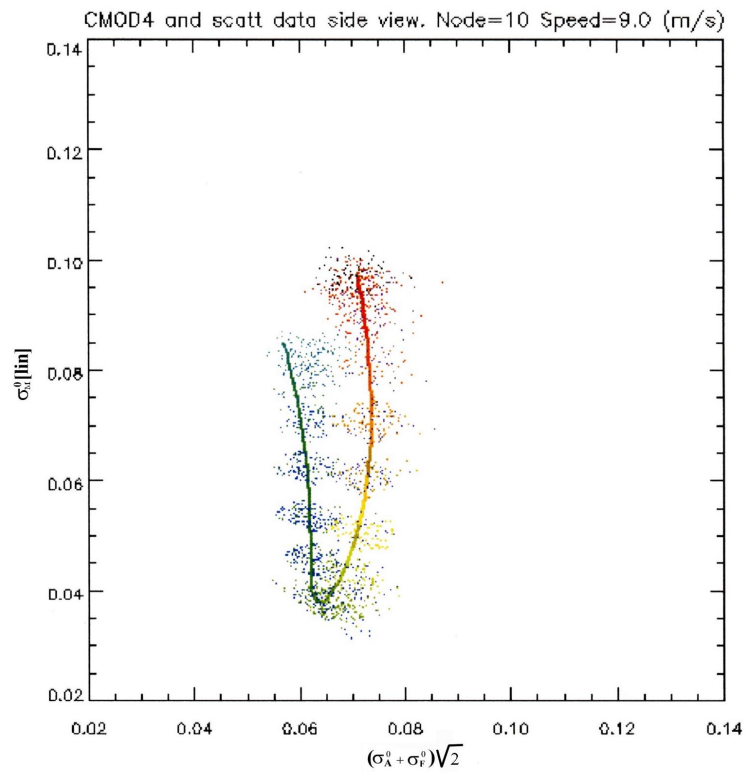


Fig. 1.10: section of CMOD4 and σ^0 measurements for node 10 and wind speed of 9 m/s on the plane $\sigma_A^0 = \sigma_F^0$.

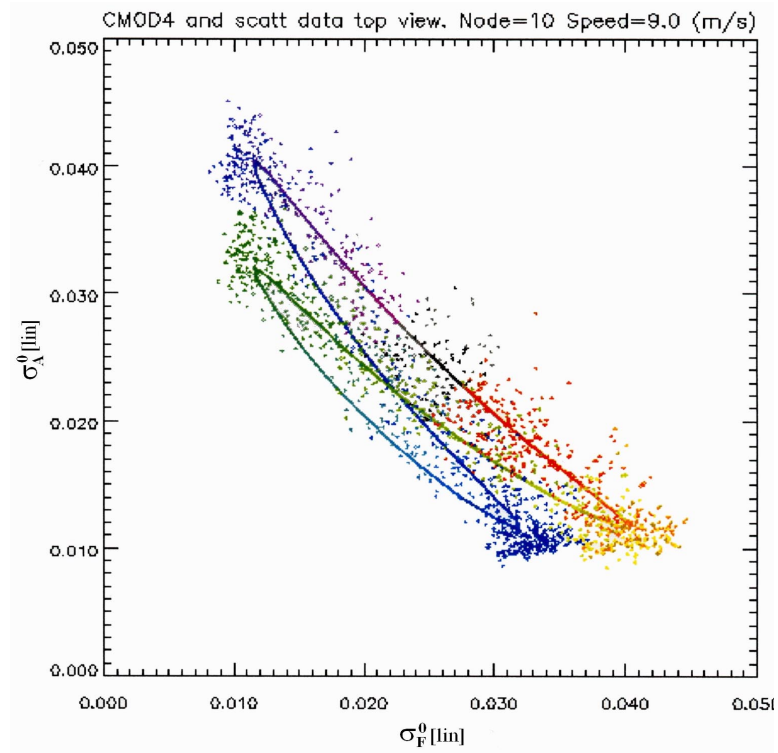


Fig. 1.11: section of CMOD4 and σ^0 measurements for node 10 and wind speed of 9 m/s on the plane $\sigma_A^0 \sigma_F^0$.

Now we consider an orthogonal section relevant to node 10. This is a section on the plane $\sigma_F^0 + \sigma_A^0 = 2\sigma_{ref}^0$ and is plotted on the plane $\left[(\sigma_A^0 - \sigma_F^0) / \sqrt{2}; \sigma_M^0 - \overline{\sigma_M^0} \right]$. At different values of σ_{ref}^0 different wind speeds are selected.

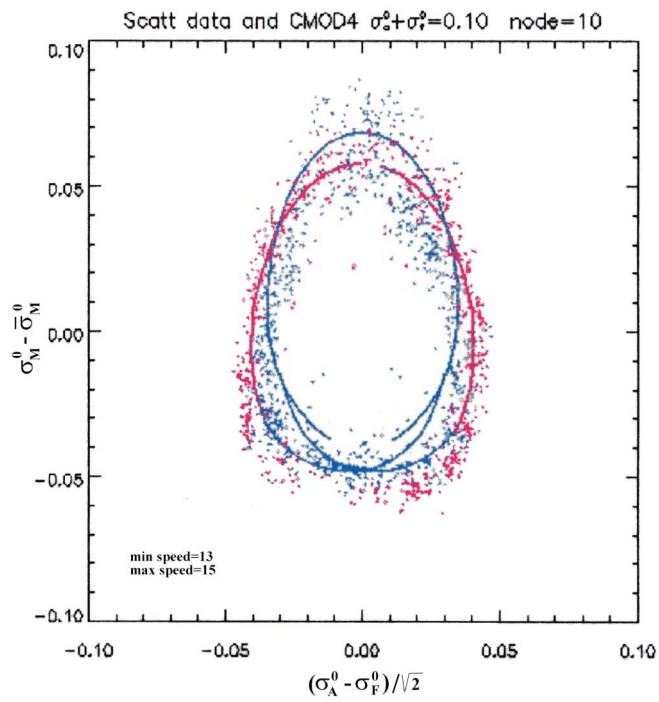


Fig. 1.12: section of CMOD4 and σ^0 measurements for node 10 in the plane $\sigma_A^0 + \sigma_F^0 = 0.10$

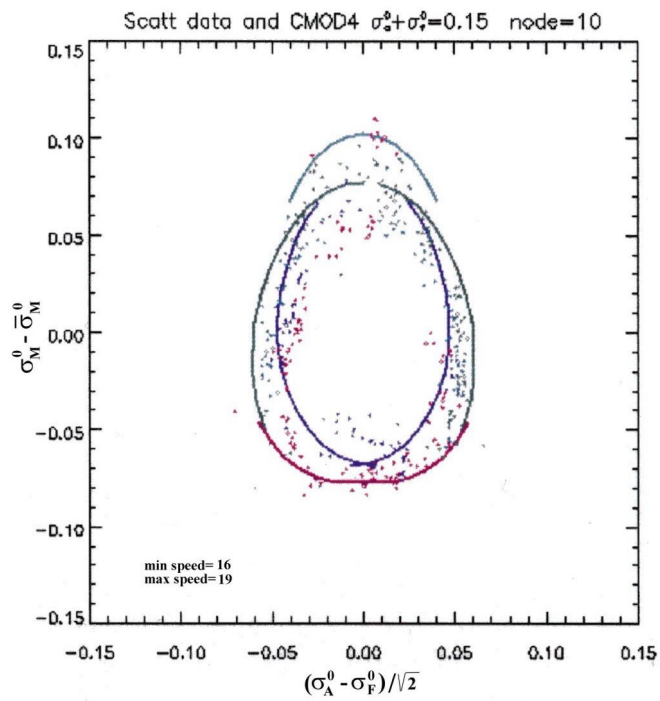


Fig. 1.13: section of CMOD4 and σ^0 measurements for node 10 in the plane $\sigma_A^0 + \sigma_F^0 = 0.15$

We can say that for lower wind speed in the section fall many points that lie quite well the model. For high wind speed data is more scattered.

After these analyses we can settle that high speed measurements stray greater from the model, so they are less reliable and we can confirm that it's necessary a study to recalibrate the model for these speeds.

It seems so necessary a revision of the model and a correction as it can't provide correct wind field.

To extend the model to high wind speed it will be better to work with high wind speed scatterometer data set but it's difficult to recognise these areas of the ocean surface, as they are limited. So it's better to refer to particular atmospheric events characterized by strong wind and to use these phenomena to work, such as tropical cyclones.

CHAPTER 2

TROPICAL CYCLONE

A tropical cyclone (TC) is a low pressure system that forms in the tropics, which has a well defined cyclone surface wind circulation and high wind velocity [Holland, 1993]. Structurally, TCs have their strongest winds near the earth's surface.

Tropical cyclones vary in both size and intensity. The diameter can vary from 60 to 300 nm (nautical miles) but both large and small cyclones can have devastating wind speed near the centre.

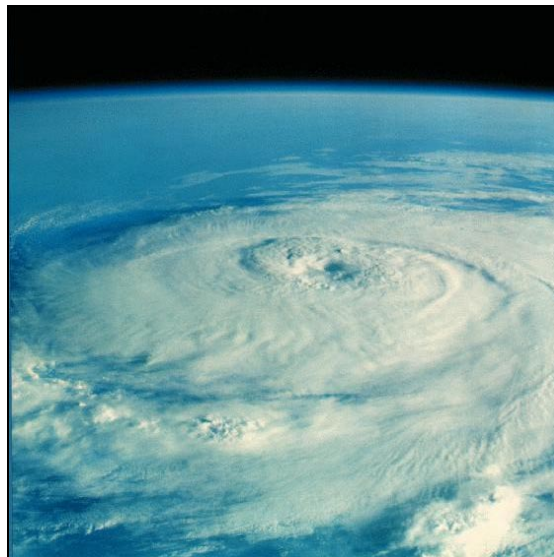


Fig. 2.1: Hurricane Elena in the North Atlantic Ocean 1985 [www.nasa.gov].

TC owe their violence to the enormous amount of heat energy released by the condensation and precipitation of the water vapour contained in the rising moist and convectively unstable tropical and equatorial air masses.

Tropical cyclones therefore can develop only in the presence of hot, moist, and convectively unstable air in those sections of tropical and equatorial regions where the deflecting force is sufficiently intense to transform convergence into cyclonic circulation.

The action of deflecting force caused by the rotation of the Earth enhances their intense cyclonic circulation.

The cyclone is characterized by three distinctive parts: the eye, the eyewall and spiral rain bands.

The eye is located in the centre of the tropical cyclone and is produced by intense spiralling of the storm. It's composed of air that is slowly sinking and sky clears and calm and the lowest surface pressure characterize it. The eye is surrounded by an eyewall that is the area of highest surface winds. Spiral rain bands surround TCs. These are bands of heavy convective showers that spiral inward toward the storm's centre. So we can say that wind velocity in a TC section grows near the eyewall and then falls drastically in the eye. In Fig. 2.2 is a wind velocity profile in a hurricane.

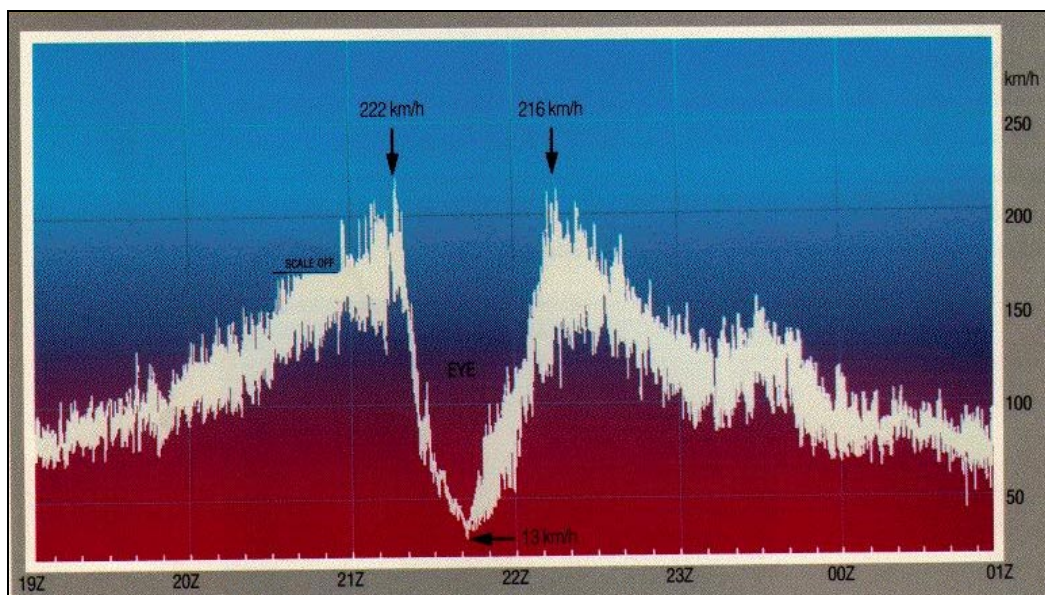


Fig. 2.2: Wind velocity recorded during the passage of hurricane Celia in Texas.

In a stationary cyclone the wind circulation is nearly circular and symmetrical. Winds blow anti-clockwise in the northern hemisphere and clockwise in the southern one. The reason is that the earth's rotation sets up an apparent force, called the Coriolis force, that pulls the winds to the right in the northern hemisphere (and to the left in the southern one). So when a low pressure starts to form north of the equator, the surface winds will flow inward trying to fill in the low and will be deflected to the right and a counter-clockwise rotation will be initiated. The opposite will occur south of the equator.

In a moving cyclone, however, the cyclonic circulation and the translator movement of the cyclone centre combine to produce stronger winds on the right side of the storm (defined with respect to the storm's motion). This is because the TC moving velocity is added to the wind velocity.

A TC with 90 mph while stationary would have winds up to 100 mph on the right side and only 80 mph on the left side if it began moving at 10 mph (Fig. 2.3).

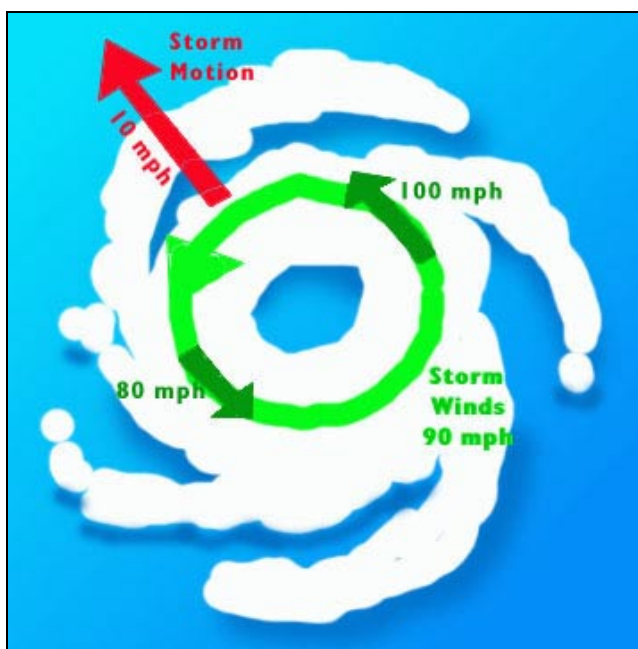


Fig. 2.3: wind velocity in a TC in the northern hemisphere [www.noaa.gov].

Note that forecasting centre advisory takes this asymmetry into account and would state that the highest winds were 100 mph. For TC in southern hemisphere these differences are reversed: the strongest winds are on the left side of the storm.

CHAPTER 3

EXPERIMENTS

3.1: PREMISE

It is well known that the CMOD4 model is not suitable when high wind speeds are in question and this is a fundamental fact to be considered when TCs want to be detected. It has been shown that in the case of extreme events the scatterometer wind speeds are underestimated [Quilfen et al., Yueh et al., Donnelly et al.]. In particular it has been proved [Quilfen et al.] that, both in the C-band and Ku-band cases, for wind speeds greater than 20 m/s the scatterometer wind speeds are inaccurate. In general it has been postulated [Donnelly et al.] that the principle error sources that limits the scatterometric performances for high wind speeds are:

- 1) the deficiency of the GMF;
- 2) the volume scattering caused by the rain drops and the surface roughness generated by the rain;
- 3) the high wind gradient within a resolution cell near the eyewall where the maximum wind speeds are expected.

In the following, in accordance to what accomplished in the most recent studies [Yueh et al., Stoffelen et al.] (unavailable to the authors at the time this work has been conducted) we concentrate on the GMF modelling as major fact to be analyzed to improve the quality of TC wind speed estimation.

3.2: THEORETICAL FACTS

In this chapter we describe the study we have performed in order to examine the relationship between the measured σ^0 and the independently measured V (wind speed). Although this may sound very easy in principle this is actually not at all a trivial task. In fact, within a TC the wind speed can reach 50-60 m/s and for this velocity is not possible to perform in situ measurements. In order to overcome such a major drawback we use the Holland hurricane model [Holland, 1980] to estimate the independent wind speed 3D pattern. The model parameters are estimated by making use of meteorological warning issued by forecast centres.

According to the Holland model, a wind speed profile, i.e. a cut of the 3D wind speed pattern, is described as follows [Holland, 1980]:

$$V(r) = \left[AB(p_n - p_c) \frac{\exp(-A/r^B)}{\rho r^B} \right]^{1/2}, \quad (12)$$

where r is the distance from the cyclone centre, ρ is the air density (assumed constant and equal to 1.15 kg/m³), p_n is the ambient pressure (theoretically at infinite radius, in practice, the value of first anticyclonically curved isobar) and p_c the central pressure (mb). As r goes to infinity the wind speed goes to 0 as expected. A and B are positive scaling parameters that are related to the radius of maximum wind speed by the relation [Holland, 1980]:

$$R_{\max} = A^{1/B}. \quad (13)$$

As B increases, the eye expands, the pressure drop is larger and the wind field adjust to give stronger winds near the centre and weaker winds at larger radii (Fig.3.1, 3.2).

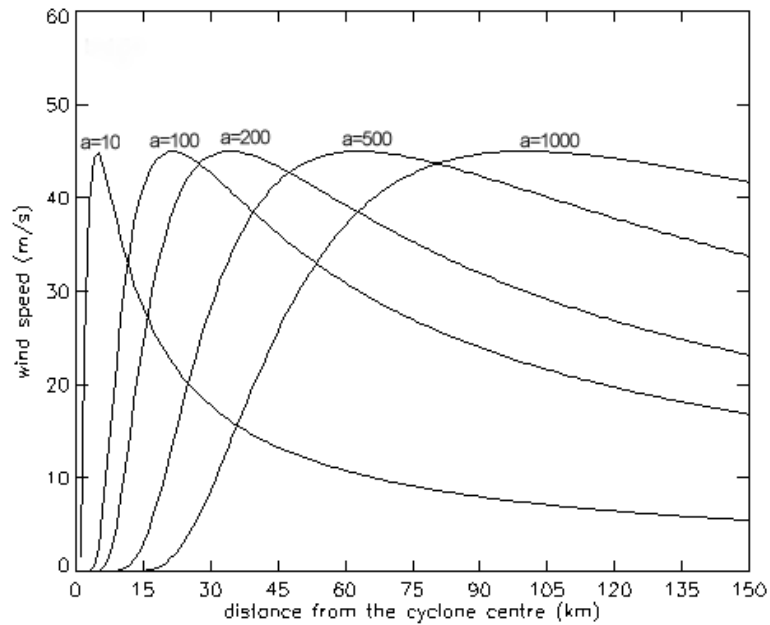


Fig. 3.1: The Holland hurricane model at variance of the parameter A..

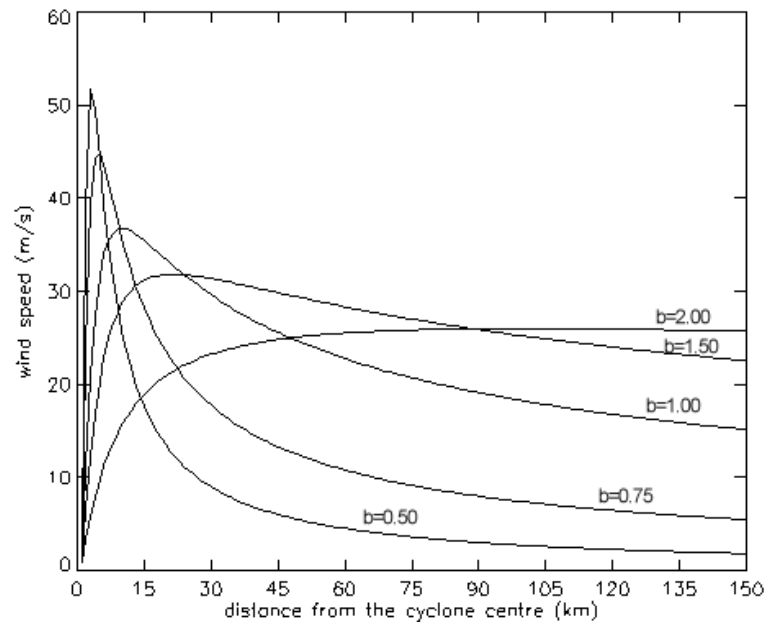


Fig. 3.2: The Holland hurricane model at variance of the parameter B .

As show in the previous figures we physically have that A determines the location of V_{\max} relative to the origin (Fig. 3.1) and B defines the shape of the profile (Fig. 3.2).

We note also that V_{\max} is given by [Holland, 1980]:

$$V_{\max} = C(p_n - p_c)^{1/2} , \quad (14)$$

in which

$$C = \left(\frac{B}{\rho e} \right)^{1/2} . \quad (15)$$

Pressure observations are generally more stable than wind ones but they are not always available in a TC meteorological warning. Conversely, wind values are always available for a TC. As a matter of fact in this work as first approach we have chosen to fit the model by means of wind speed measurements only.

Accordingly we had better rewrite the Holland model noting that

$$(p_n - p_c) = \frac{V_M^2}{D^2} , \quad (16)$$

and

$$D^2 = \frac{B}{\rho e} , \quad (17)$$

hence

$$V(r) = \left[\frac{AeV_M^2}{r^B} \exp(-A/r^B) \right]^{1/2} . \quad (18)$$

This model can be applied to each TC, at variance of the parameters, to estimate the hurricane 3D wind speed pattern. In fact, in the case of symmetric TC, once A and B and V_{max} are properly chosen the wind speed can be obtained as function of the distance from the cyclone centre. Since it is expected to know V_{max} the free parameters to be estimated are A and B . An estimate of A and B can be accomplished performing a model fitting versus some wind speed measurements.

However in real cases symmetrical TC wind speed patterns are not appropriate. To best follow the asymmetrical wind speed pattern of a TC V_{max} , A and B must be meant as angular functions.

In practice only the overall V_{max} can be at disposal and therefore three free parameters, i.e. V_{max} , A , B , must be estimated for each wind speed profile.

In our analysis a four quadrant study has been conducted. As a matter of fact, the wind speed data made available by the meteorological forecasts centers reports are detailed for each quadrant.

In particular, in a National Hurricane Centre report, for each quadrant, among various information, are provided the distances from the centre (in nautical miles, see nm in Table 3.1) at which the 34, 50, 64 kt wind speeds are given.

```

ZCZC MIATCMAT5 ALL
TTAA00 KNHC DDHMM
HURRICANE DENNIS FORECAST/ADVISORY NUMBER 23
NATIONAL WEATHER SERVICE MIAMI FL AL0599
1500Z SUN AUG 29 1999

HURRICANE CENTER LOCATED NEAR 30.4N 78.5W AT 29/1500Z
POSITION ACCURATE WITHIN 30 NM

PRESENT MOVEMENT TOWARD THE NORTH OR 355 DEGREES AT 9 KT

ESTIMATED MINIMUM CENTRAL PRESSURE 971 MB
EYE DIAMETER 30 NM
MAX SUSTAINED WINDS 90 KT WITH GUSTS TO 110 KT
64 KT..... 75NE 60SE 50SW 50NW
50 KT.....125NE 125SE 75SW 100NW
34 KT.....150NE 140SE 100SW 140NW
12 FT SEAS..200NE 150SE 150SW 200NW
ALL QUADRANT RADII IN NAUTICAL MILES

REPEAT...CENTER LOCATED NEAR 30.4N 78.5W AT 29/1500Z
AT 29/1200Z CENTER WAS LOCATED NEAR 30.0N 78.4W

FORECAST VALID 30/0000Z 31.7N 78.5W
MAX WIND 90 KT...GUSTS 110 KT
64 KT... 75NE 60SE 50SW 50NW
50 KT...125NE 125SE 75SW 100NW
34 KT...150NE 140SE 100SW 140NW

FORECAST VALID 30/1200Z 33.0N 77.5W
MAX WIND 95 KT...GUSTS 115 KT
64 KT... 75NE 60SE 50SW 50NW
50 KT...125NE 125SE 75SW 100NW
34 KT...150NE 140SE 100SW 140NW

FORECAST VALID 31/0000Z 34.0N 76.0W
MAX WIND 100 KT...GUSTS 120 KT
64 KT... 75NE 60SE 50SW 50NW
50 KT...125NE 125SE 75SW 100NW
34 KT...150NE 140SE 100SW 140NW

```

Table 3.1: NHC warning of cyclone Dennis - 29/8/1999 15:00
[www.nhc.noaa.gov].

For each quadrant to perform the Holland model parameters estimation the wind speed data set has been enriched by a wind speed retrieved from scatterometer data once ensured that this wind speed is below 15 m/s. Of course following such a quadrant approach unnatural discontinuities into the 3D wind speed pattern arise.

In order to smooth them a weighted averaging has been performed. In order to take into account the usual ERS-2 scatterometer σ^0 filtering an Hamming filtering over the 3D wind speed Holland-based pattern has been applied. We note however that this procedure is questionable since the relationship between the V and the σ^0 is non-linear. A more precise approach requires to transform the 3D wind speed pattern in terms of σ^0 and then to apply the customary Hamming filtering. Unfortunately this latter approach calls for the knowledge of the GMF, which is in fact object of this study. As a matter of fact, an iterative procedure must be considered and the approach we have considered in this piece of work can be meant as the first step of this iterative procedure. This fact is going to be furthered in the future.

All this matter has been applied over a set of cyclones selected according to the following specific criteria:

- 1) the availability of ERS-2 scatterometer measurements in 1999 and 2000;
- 2) the availability of scatterometer measurements of at least 2/3 of the cyclone structure;
- 3) a maximum temporal span between the scatterometer measurements and the reference time of the meteorological warning of 2 hours has been considered;
- 4) the existence in the warning of at least three wind speed data for each cyclone quadrant.

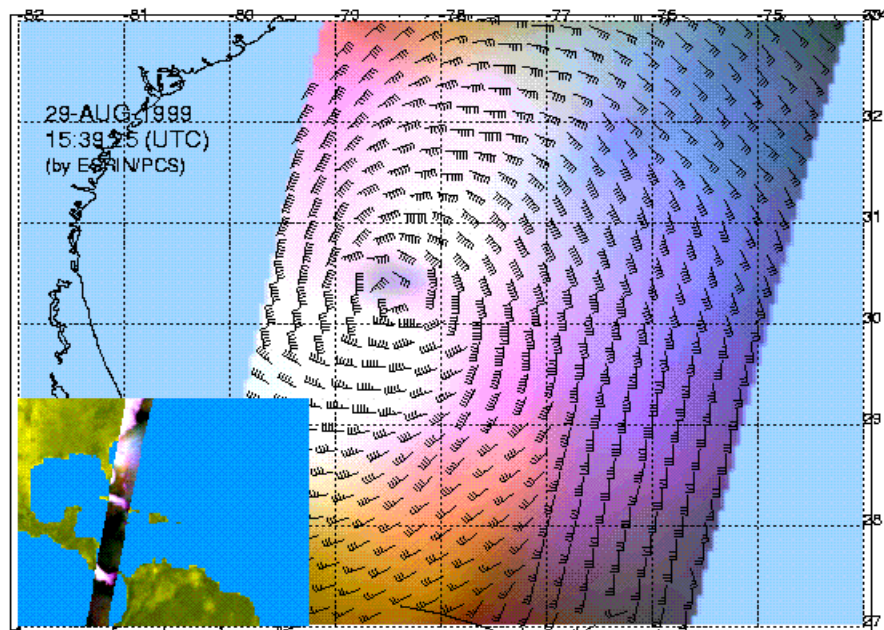


Fig. 3.3: The cyclone Dennis as observed by the ERS-2 scatterometer. In the inset the satellite track over the cyclone is shown.

For each quadrant, the additional wind speed data used to estimate the Holland model parameters has been chosen among the wind field retrieved by means of the scatterometer data:

- 1) the Holland model best fits up to 200 to 300 km from cyclone centre;
- 2) the CMOD4 GMF is capable to best match wind speed below 15 m/s;
- 3) this additional wind speed is searched at a TC centre distance located in the 250-300 km range in order to best provide an independent measurement.

3.3 EXPERIMENTAL FACTS

In this section we detail the experiments conducted according the rationale described in .

First of all we had to select a proper set of TCs.

As a result of the first selection we have found 16 cyclones. Unfortunately, only for 11 of them it was possible to find the additional wind speed point according to the requirements detailed in Chapter.

A first analysis of these latter TCs suggested considering 6 of them as the most appropriate.

They are listed in Table 3.2.


NAME	DATE	FORMATION ZONE	SYMBOL LIST
Beatriz	11 July 1999	North East Pacific	*
Cindy	26 august 1999	Atlantic	
Daniel	29 July 2000	North East Pacific	Δ
Dennis	29 august 1999	Atlantic	\diamond
Dora	12 august 1999	North East Pacific	X
Isaac	29 September 2000	Atlantic	+

Table. 3.2: Relevant to the selected cyclones.

Once that the TCs have been selected the Holland hurricane model has been applied in each quadrant. In Fig.3.4 the case of cyclone Dennis is shown with reference to the NE and SW quadrants (horizontal dotted line represents the overall V_{max} in the cyclone). This shows the suitability of the Holland model and the asymmetrical structure of the cyclone. Note also that with respect to the 3D wind speed Holland-based pattern the plot shown in Fig.3.4 is actually relevant only to NE-SW wind speed profile, see Par. 3.2.

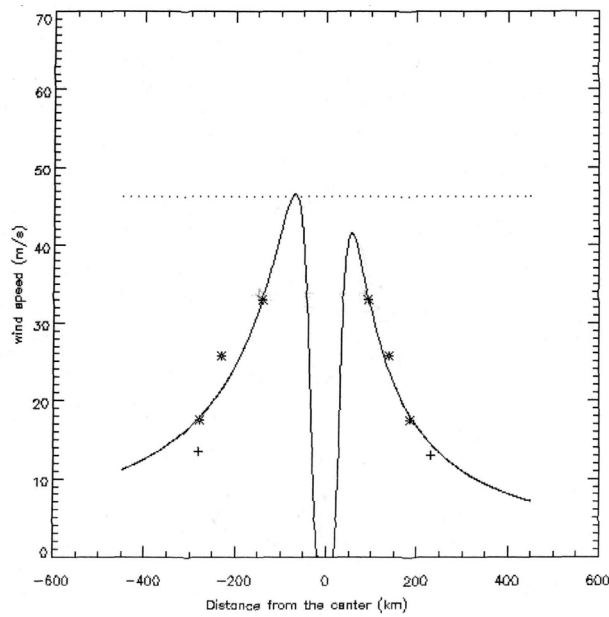


Fig.3.4: Cyclone Dennis - NE-SW wind speed profile.

Once that the quadrant-to-quadrant analysis has been performed the smoothing procedure has been applied in order to limit the occurring unnatural discontinuities in the 3D wind speed pattern, see Figs. 3.5, 3.6.

To do that a high resolution (5 km) grid of 610 x 610 km has been created. This grid is centred in the tropical cyclone centre, as indicated in the NOAA warning and is oriented like the scatterometer swath on the same area. For each node of the grid the distance from the centre is determined and, according to the model applied in each quadrant, the wind speed velocity is determined.

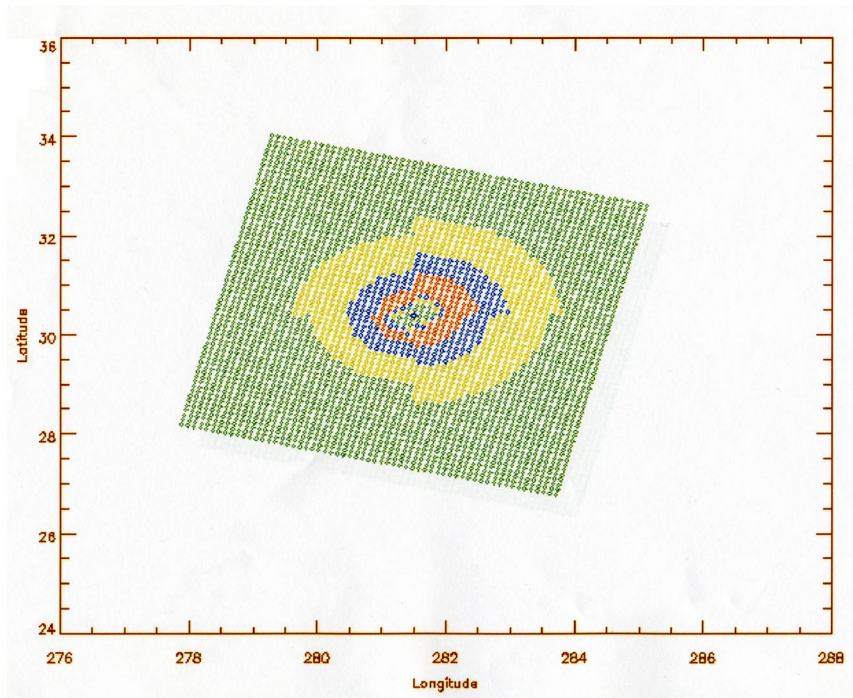


Fig. 3.5: high resolution grid with wind speed for Cyclone Dennis. Each colour is linked to a wind speed range. Green: $v < 20$ m/s; yellow: $20 \leq v < 30$; blue: $30 \leq v < 40$; red: $v \geq 40$ m/s.

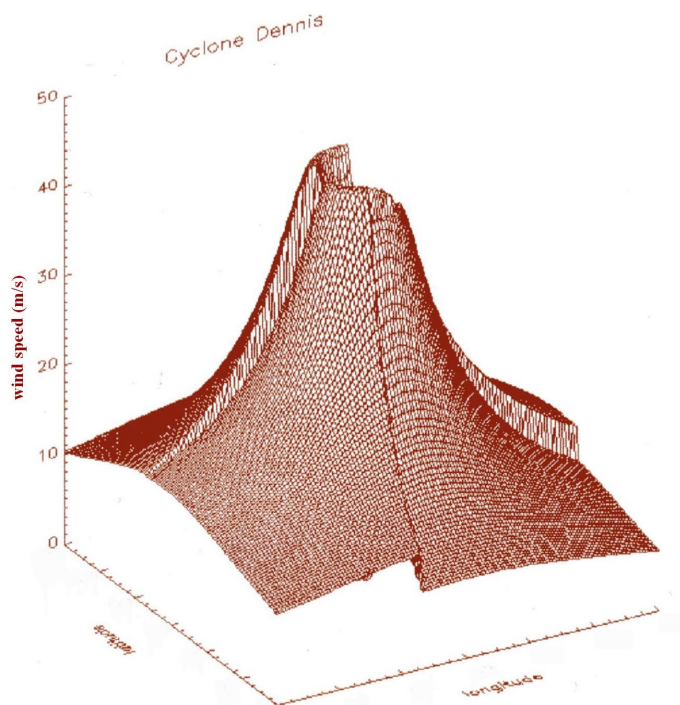


Fig.3.6: the cyclone Dennis 3D wind speed pattern before.

In Fig.3.7 the corresponding 3D smoothed wind speed pattern is shown.

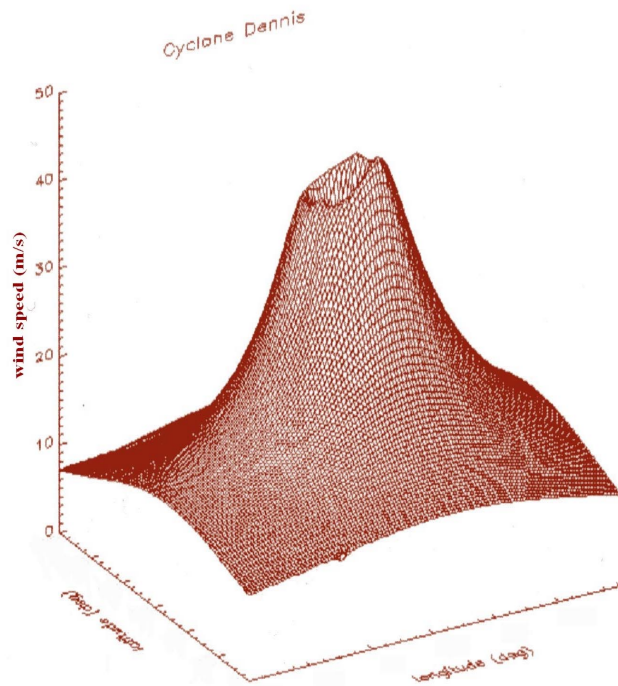


Fig.3.7: The cyclone Dennis 3D wind speed pattern after smoothing.

After we apply the Hamming filtering so we obtain a 3D wind speed pattern accordingly to the scatterometer resolution and it can be employed as reference.

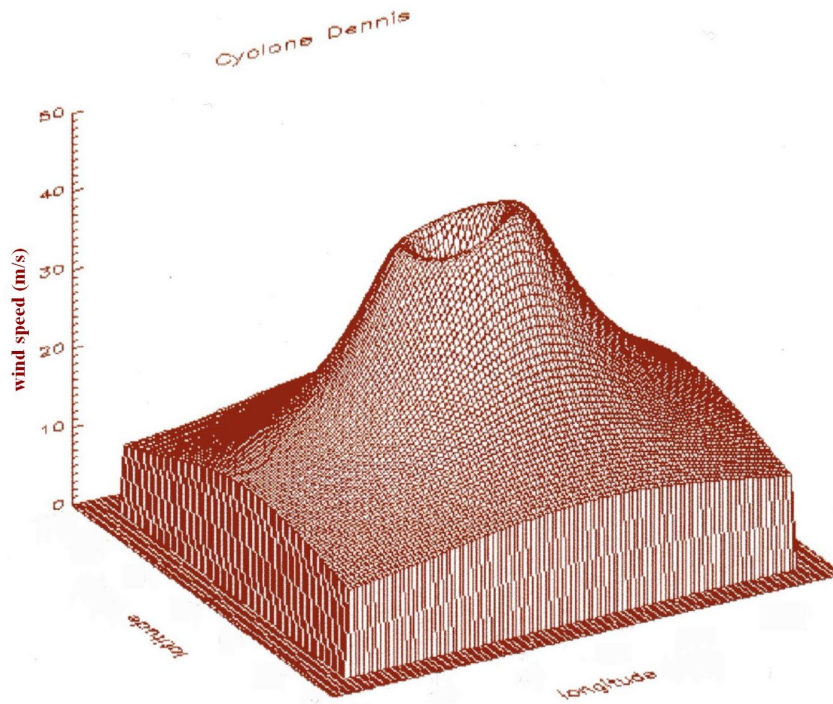


Fig. 3.8: 3D wind speed pattern after Hamming filtering.

For each node of the scatterometer grid node three backscattering measurements (σ_M^0 , σ_F^0 , σ_A^0) are available but the corresponding incidence angles are different. Since the CMOD4 GMF is incident angle θ and wind direction φ dependent we fixed them in the following figure format, see Figs. 3.9-3.18. These figures show σ^0 vs. V where σ^0 is relevant to the scatterometer measurements and V to the 3D Holland-based wind speed pattern. The colour format is such that a principal colour is associated to each antenna (red=*fore*, green=*mid*, blue=*aft*) and the symbols are relevant to the cyclones according to Table 3.2. The continuous curve refers to the corresponding CMOD4 GMF.

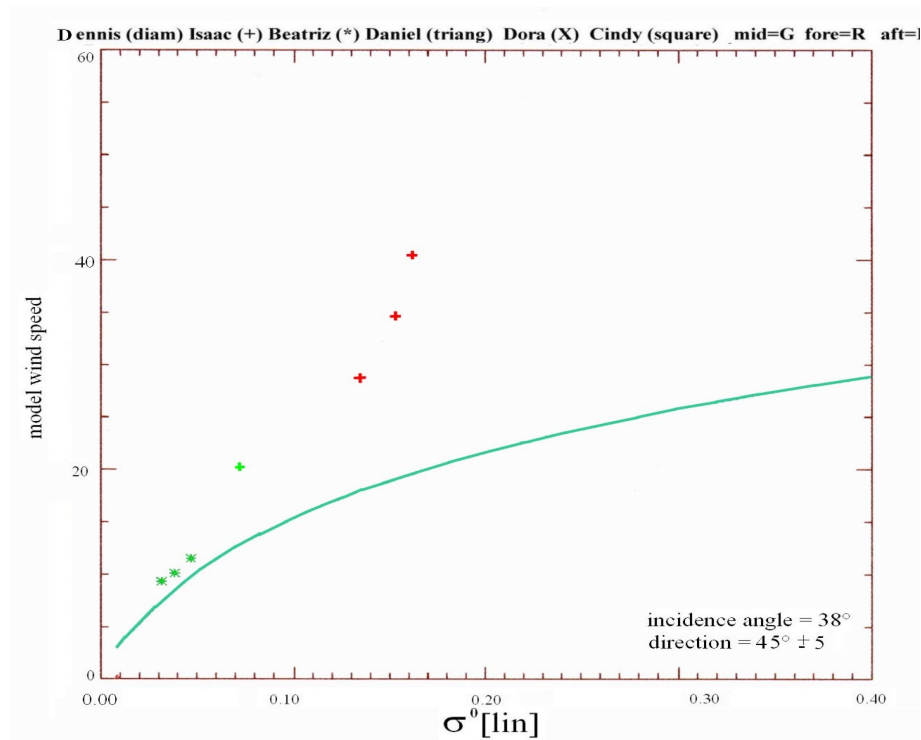


Fig.3.9: wind speed with respect to σ^0 for incidence angle of 38° and wind direction range of 40° - 50° .

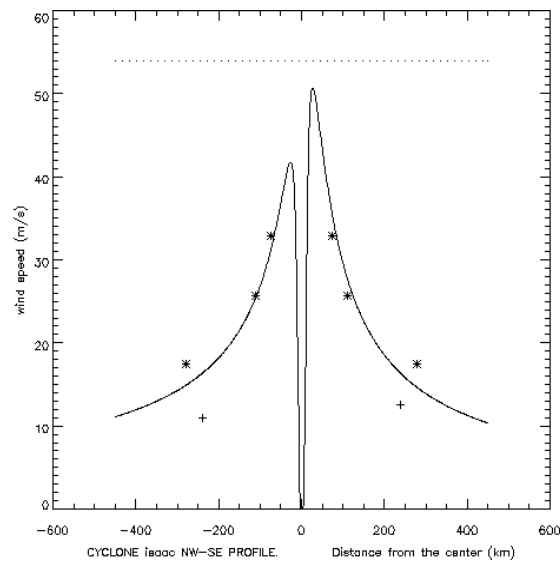


Fig.3.10: Cyclone Isaac - NW-SE wind speed profile.

In particular, in Fig.3.9 the case of θ equal to 38° and φ equal to $45^\circ \pm 5^\circ$ is shown. We note that for low wind speeds the GMF agreement with the Holland wind speeds is, as expected, obtained. This is untrue for high wind speeds. In this case we also have an unexpected and significant discrepancy for a point referring to a wind speed values of about 20 m/s and pertaining to the Isaac cyclone. Other similar problems have been encountered with the Isaac cyclone. This may be explained thinking that the relevant 3D Holland-based wind speed pattern is not best tailored for low and moderate wind speeds. As a matter of fact, if we move back to the NW-SE Holland wind speed profile (Fig.3.10) we have that according to the fitting for low and moderate wind speed the Holland profile does not fit adequately the wind speeds estimated through the scatterometer. If we assume that these latter wind speeds can be considered precise in this wind speed range this can be due to the uncertainties in the wind speed TC warning reports and/or to the Holland model itself.

Before proceeding further we note that a saturation effect appears and this has been experienced also in other cases not shown. This fact is in agreement to what stated in Donnelly et al.

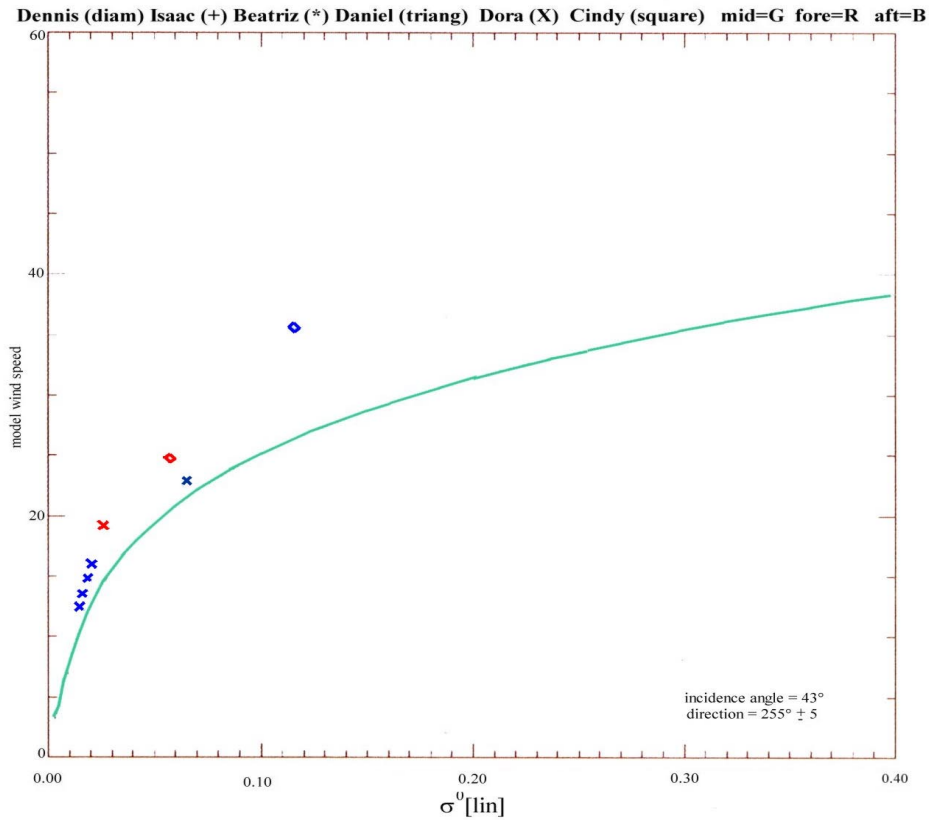


Fig.3.11: wind speed with respect to σ^0 for incidence angle of 43° and wind direction range of 250°-260°.

In Fig.3.11 the case of θ equal to 43° and φ equal to 255° ± 5° is shown. Again we have that results are dependent on the specific cyclone, i.e. to the relevant 3D Holland-based wind speed pattern and on the wind speed.

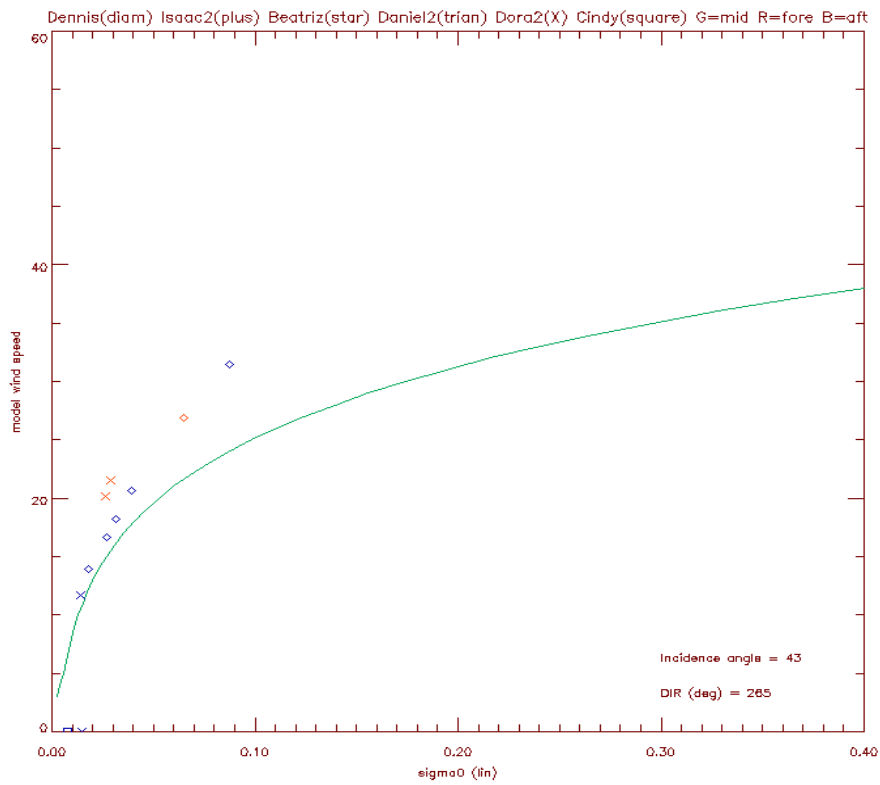


Fig.3.12: wind speed with respect to σ^0 for incidence angle of 43° and wind direction range of 260° - 270° .

In Fig.3.12 the case of θ equal to 43° and φ equal to $265^\circ \pm 5^\circ$ is shown.

Comments similar to the former cases can be made.

In the next figures we have results for other incidence angle and wind directions.

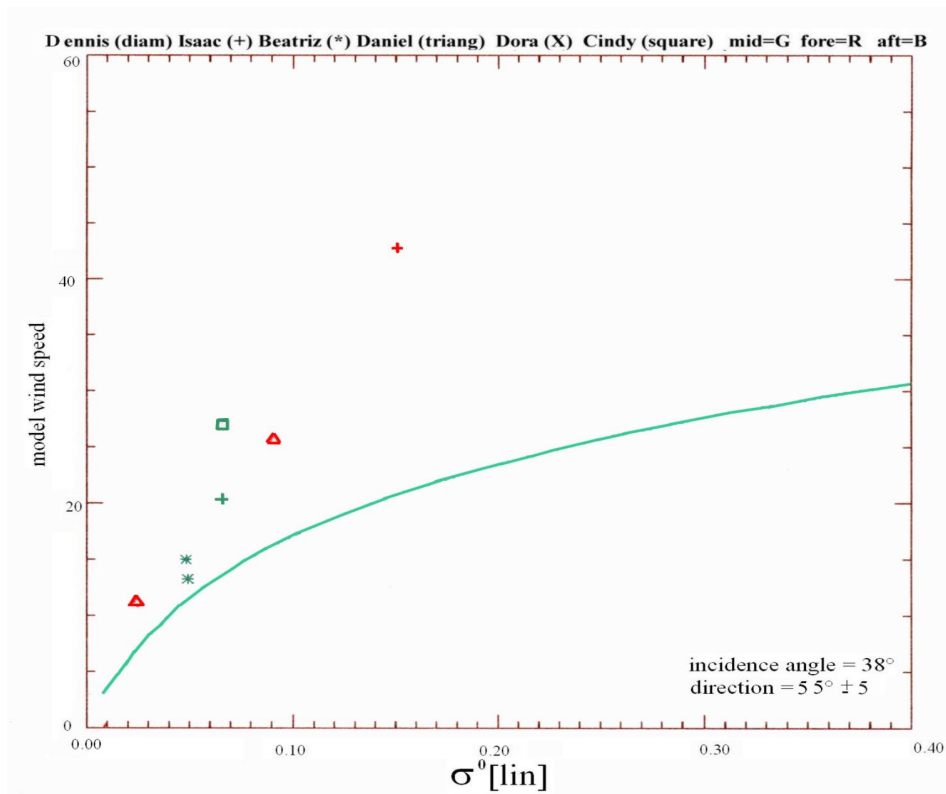


Fig.3.13: wind speed with respect to σ^0 for incidence angle of 38° and wind direction range of 50°-60°.

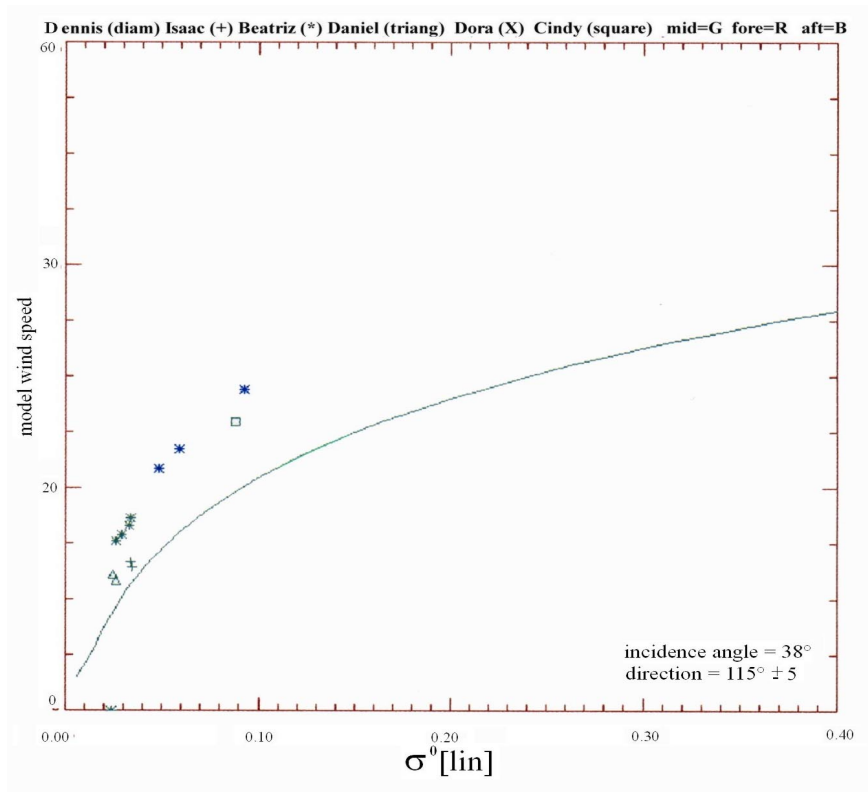


Fig.3.14: wind speed with respect to σ^0 for incidence angle of 38° and wind direction range of 110°-120°.

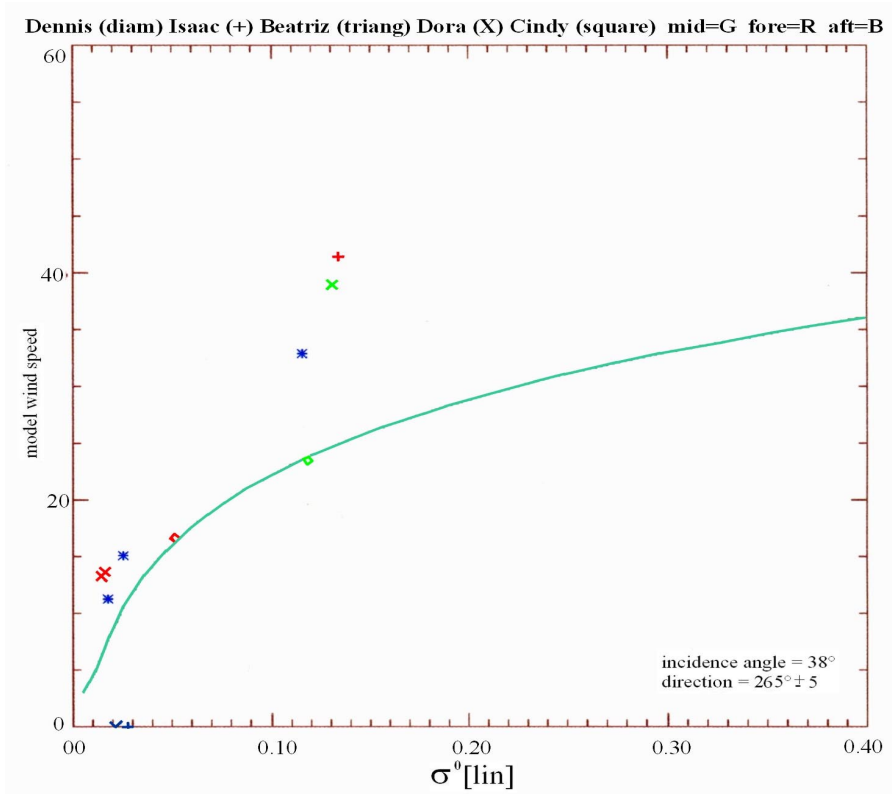


Fig.3.15: wind speed with respect to σ^0 for incidence angle of 38° and wind direction range of 260°-270°.

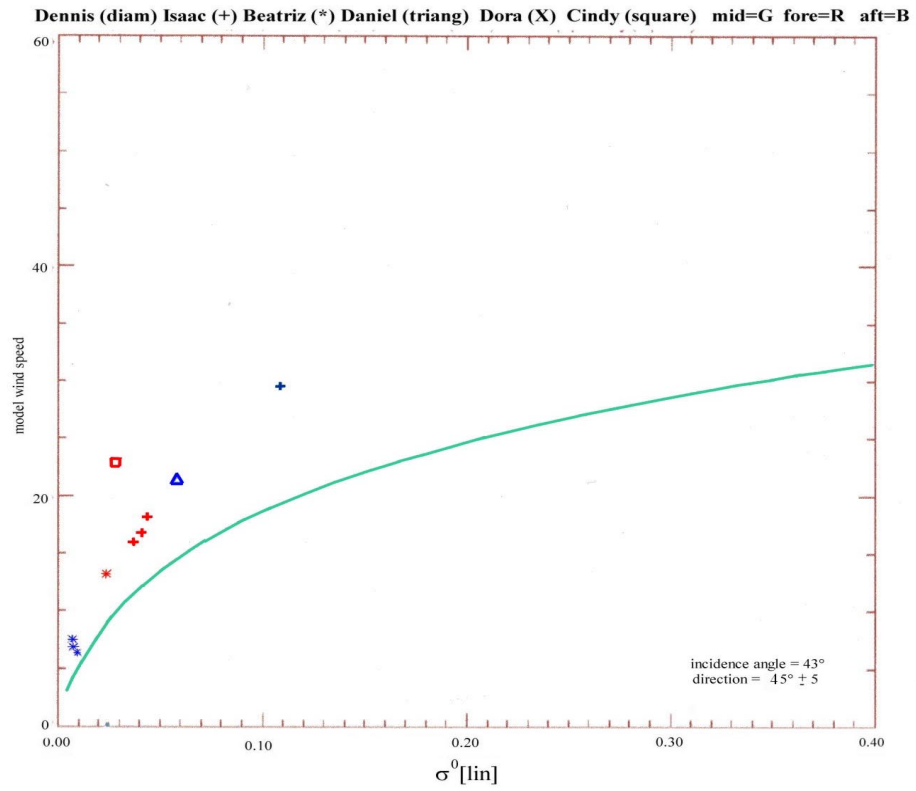


Fig.3.16: wind speed with respect to σ^0 for incidence angle of 43° and wind direction range of 40°-50°.

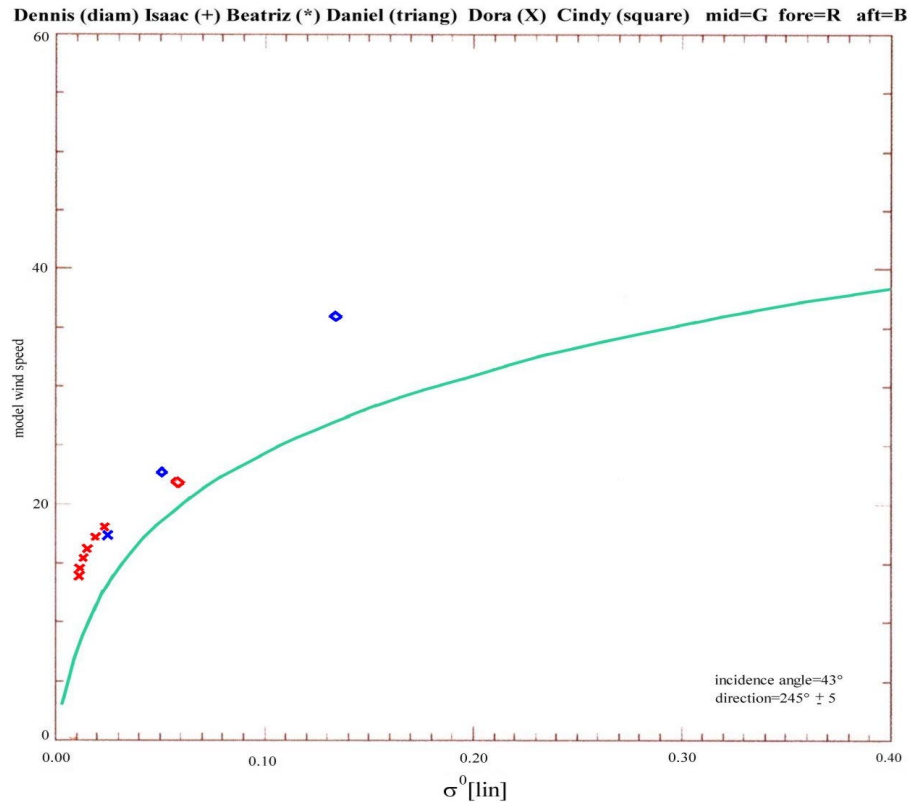


Fig.3.17: wind speed with respect to σ^0 for incidence angle of 43° and wind direction range of 240°-250°.

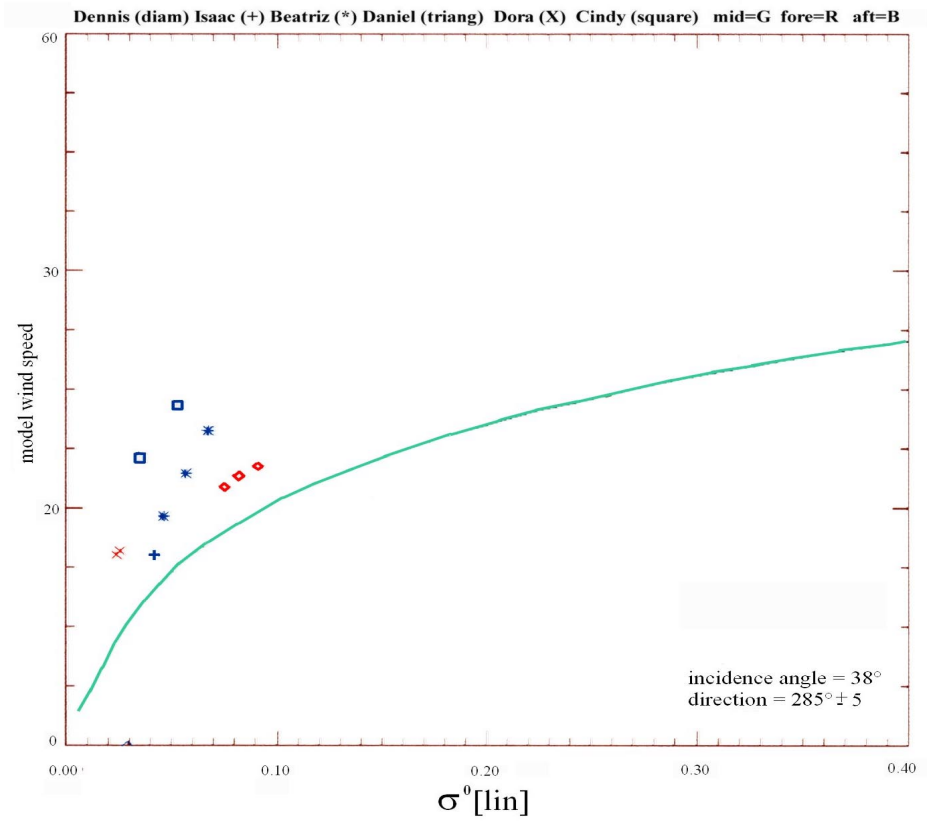


Fig.3.18: wind speed with respect to σ^0 for incidence angle of 38° and wind direction range of 280°-290°.

CHAPTER 4

CONCLUDING REMARKS

A study regarding the estimation of wind speeds through scatterometer measurements have been conducted. The study has been based on the Holland hurricane model and the ERS-2 C-band scatterometer. The first results that have been obtained are not always straightforward to be physically interpreted but some conclusions can be drawn as hints of future activity. The CMOD4 underestimates the high wind speeds. The relevant geophysical relationship that can be figured out by these experiments is obviously dependent on the incidence angle and wind direction but also on the considered cyclone. This fact can be both justified in terms of the cyclone structure variability and in terms of the Holland hurricane model. In general the data at the input of the Holland model may be critical as well as its use to obtain a 3D wind speed pattern.

Finally we have to note that some interesting papers on this subject have been recently published and made available to the authors after this piece of work has been completed. With respect to the paper of Yueh et al. we note that in our case the GMF to high wind speed regimes seems to have a more involved functional form than a simple linear one. Although, as suggested in the paper of Yueh et al., an analysis of the concurring rain effects is appropriate. With respect to the paper of Stoffelen and deHaan and references therein we note that also in our experiments we have experienced a saturation behaviour at high wind speed regimes. Further the use of the new CMOD5 GMF developed in Stoffelen and deHaan

should be considered in the development of this piece of work. We note in fact that the rationale underlying this study is similar to the one of Yueh et al. [Yueh et al., 2001] and therefore independent of the one of Stoffelen and deHaan [Stoffelen, de Haan, 2001].

REFERENCES

- Donnelly, W.J., J.R.Carswell, R.E.McIntosh, P.S.Chang, J.Wilkerson, F.Marks, P.G.Black, "Revised Ocean Backscattering Models and Ku Band under High-Wind Conditions", *J. Geophys. Res.*, vol.103, no.C5, pp.11485-11497, May 1999.
- Garbell, M.A., *Tropical and Equatorial Meteorology*, Pitman
- Holland, G.J., "An Analytical Model of the Wind and Pressure Profiles in Hurricanes", *Mon. weath. Rev.*, vol.108, pp.1212-1218, 1980.
- Lecomte, P., The ERS Scatterometer instrument and the On-Ground processing of its Data, *Proceedings of Emerging Scatterometer Applications-from Research to Operation*, 1998 ESTEC, The Netherlands
- Yueh, H., B.W.Stiles, W.Tsai, H.Hu, W.T.Liu, "QuickSCAT Geophysical Model Function for Tropical Cyclones and Application to Hurricane Floyd", *IEEE Trans. on Geoscience and Remote Sensing*, vol.39, no.12, pp.2601-2612, Dec.2001.
- Quilfen, Y., B.Chapron, T.Elfouhaily, K.Katsaros, J.Tournadre, "Observation of Tropical Cyclone by High-Resolution Scatterometry", *J. Geophys. Res.*, vol.103, no.C4, pp.7767-7786, Apr.1998.
- Stoffelen, A., "Scatterometry", Ph.D. Dissertation, University of Utrecht, Utrecht, The Netherlands, 1998.
- Stoffelen, A., S.deHaan, "CMOD5", SAF/OSI/KNMI/TEC/TN/140 report, Nov.2001.
- www.nhc.noaa.gov